HOSTED BY

ELSEVIER

Available online at www.sciencedirect.com

ScienceDirect

Journal of Magnesium and Alloys 5 (2017) 412–422
www.elsevier.com/journals/journal-of-magnesium-and-alloys/2213-9567

Full Length Article

Durability of AZ31 magnesium biodegradable alloys polydopamine aided: Part 1

Tullio Monetta [a,*], Annalisa Acquesta [a], Anna Carangelo [a], Nicola Donato [b], Francesco Bellucci [a]

[a] Department of Chemical Engineering, Materials and Industrial Production, University of Napoli Federico II, Piazzale Tecchio 80, 80125 Napoli, Italy
[b] FCA Italy – Avvocato Giovanni Agnelli Plant, Via San Paolo 67/71, 10095 Grugliasco (TO), Italy

Received 12 July 2017; accepted 29 September 2017

Available online 22 November 2017

Abstract

The use of magnesium alloys, as a biodegradable medical device, is an interesting challenge for the biomaterials field. Its rapid degradation and the release of hydrogen, when exposed to biological fluids, are the main drawbacks for clinical applications. In this work, a coating made of polydopamine (PDOPA), is used as an intermediate layer to decrease the degradation rate of AZ31 magnesium alloy/polymeric coating system, when exposed to Hank's solution. Experimental results highlighted: (i) the formation of a thin PDOPA layer, (ii) an increased adhesion in the organic coating/metallic substrate system, (iii) a decrease of two orders of magnitude of the corrosion rate when the PDOPA film is used together with an external organic coating, (iv) the efficacy in the use of PDODA due to the synergistic effect of both, physical and chemical, interactions between the PDOPA layer and the organic coating.

Keywords: AZ31; Polydopamine; Biodegradable alloy; Roughness; Electrochemical characterization; Medical device

1. Introduction

Metallic materials are widely employed in the production processes of medical devices like prosthesis and implants. At the beginning of the 20th century noble metals were used, nowadays, stainless steel and alloys containing tantalum, cobalt, chromium, titanium are commonly utilized. It is well known that items made of these types of metals are safely and efficiently employed in manufacturing medical devices that are left in the human body for a prolonged period due to their limited interactions with the organic tissues. Depending on the functions that the device should perform, a stronger or weaker interaction with the human body can be required. Two cases can be considered: (i) materials showing few interactions with the tissues that need to be modified to increase their response to biological fluids and (ii) highly reactive materials, for which the interactions have to be reduced.

Commercially pure (CP) titanium or titanium alloys implants fall in the first case. In fact, for some uses, a rapid osseointegration is required, so their surface should be modified to deposit bioactive materials [1–4]. Also, in the recent years, some kinds of surface treatments have been proposed, developing nanostructured surfaces, which could allow releasing drugs at a settled rate or possess antibacterial activity, to perform enhanced performances [5–10].

Magnesium alloys fall in the second case. They can be considered as suitable materials for all those applications requiring a temporary use of the medical device that, in many cases, should be removed when it has performed its function, such as biodegradables prosthesis, stents, bone fixation screws, plates, etc. The main limitations of the clinical use of the magnesium-based materials are their rapid degradation and the release of hydrogen during decomposition when in contact with living tissues. A great effort was placed looking to limit the degradation rate of Mg alloys, covering the substrate by using, i.e., a biodegradable polymeric coating, even if results obtained until now do not allow any practical purposes. Conversely, the main advantages of Mg are the high biocompatibility, the favorable mechanical properties and the potential application as a temporary device. Mg alloys, as corrodible materials, can intentionally avoid a second surgery, because magnesium ions released are removed through phagocytosis [11], possessing no allergic potential and causing no distinct inflammatory reactions [12].

* Corresponding author. Department of Chemical Engineering, Materials and Industrial Production, University of Napoli Federico II, Piazzale Tecchio 80, 80125 Napoli, Italy.
E-mail address: monetta@unina.it (T. Monetta).

https://doi.org/10.1016/j.jma.2017.09.006
2213-9567/

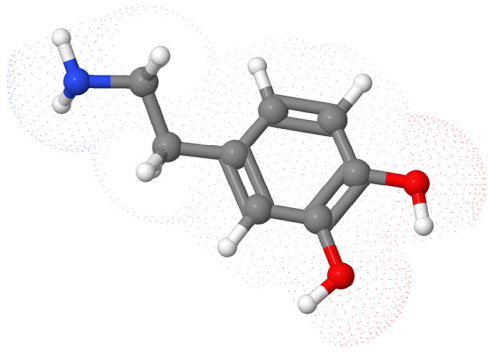

Fig. 1. Chemical structure of dopamine (CCA license of © Karl Harrison http://www.3dchem.com/).

The adjustment of Mg corrosion rate, leading to hydrogen evolution and alkalization of the site, remains the main challenge to take on. As said, a strategy to overcome this issue consists of coating the substrate by using suitable materials. Polycaprolactone (PCL) and polylactic acid (PLA), two biodegradable and biocompatible polymers, are considered to be a promising means [13–15]. Further, they are deemed to have a slow degradation rate, but the contact between the corroding metal substrate and the polymeric coating may induce their rapid degradation. Chen et al [16] show, in fact, that the locally alkaline environment, produced by the corrosion of magnesium alloy, degrades PCL and PLA, increasing the degradation rate of the substrate. A biocompatible and biodegradable coating could be interposed between the substrate and the coating, which contributes to slowing down the alloy dissolution rate, to overcome the problem. Recently, the observation of the mussels adhesion to solid surfaces has inspired the field of material science [17]. They can attach to various surfaces, ranging from natural inorganic materials (i.e. rocks) and organic materials (i.e. fish skins) to synthetic materials (i.e. Teflon) [18]. The remarkable features of mussels adhesion include the ability to achieve long-lasting adhesion in a wet environment [19].

A coating based on polydopamine (PDOPA), the principle origin of the extraordinarily robust adhesion of the mussel, could be used as an adhesive intermediate layer to increase the bonding at the interface between the metal substrate and the polymeric coating. The adhesive layer is made of dopamine, that is a catecholamine, a compound showing a primary amine functional group (Fig. 1). Dopamine is produced by several living species, in the human brain it functions as the neurotransmitter and its deficiency leads to Parkinson's disease [20].

It has been demonstrated that PDOPA coatings are biocompatible and biodegradable [21], promote cell adhesion [22] and have no cytotoxic effects [23]. Moreover, the PDOPA layer could act as an insulating layer to slow down the cathodic reaction of magnesium, that is a key factor to regulate the corrosion rate. Studies on PDOPA-based coating as efficient anchoring layer on magnesium alloy have rarely been reported until now [24–26]. To the best of our knowledge, only one paper deals with the use of polydopamine as an intermediate layer when the AZ31 alloy is used [27], while another one deals with the use of PDOPA to functionalize PCL coating [28].

Table 1
Elemental composition by weight of AZ31 magnesium alloy.

Element	Al	Zn	Mn	Si	Cu	Fe	Ni	Others	Mg
	2.5–3.5	0.7–1.3	0.2–1	0.05	0.01	>0.05	>0.05	0.4	Balance

The present work aims to test the effectiveness of the use of PDOPA in retarding the degradation rate of magnesium alloy AZ31, when exposed to Hank's solution, contributing to acquire more information on this topic.

2. Materials and methods

Sheets (130 mm × 70 mm × 3 mm) made of AZ31 magnesium alloy (Goodfellow U.K., Llangollen, UK), whose composition is reported in Table 1, were used as coupons. Dopamine hydrochloride and Trizma base, utilized in the polymerization process of PDOPA, were purchased at Sigma-Aldrich (Sigma-Aldrich, Milano, Italy). Hydrochloride acid, HCl, employed to the pretreated specimens was bought from Sigma-Aldrich (Sigma-Aldrich, Milano, Italy).

2.1. Preparation of the samples

The metallic samples were ground with SiC paper from P240 to P1200, using high purity ethanol as a lubricant, as suggested by K. Geels [29] to remove contamination layers and native oxides.

To individuate the sample's topography to be able to optimize the coating/metallic substrate adhesion and to assure the repeatability of experiments, in obtaining specimens with comparable topography, a wet chemical etching was performed, after the mechanical lapping process. The specimens were immersed in a 0.15M HCl aqueous solution, stirred at 300 rpm, for three different immersion time: 10, 30 and 60 s, respectively. The samples were, then, rinsed by using deionized water and dried in air. The acronyms used to identify the samples, obtained by the polishing and etching process, are reported in Table 2.

The comparison between the topography of the etched and lapped samples, was carried out by using only four "roughness" parameters, S_a, S_q, S_{ku} and S_{sk}, because, in our opinion, they are sufficient to distinguish quantitatively the etching treatments performed on samples and to test their repeatability [30–33]. The physical meaning of the (i) average roughness, R_a, (ii) root mean square of roughness, R_q, (iii) Kurtosis, R_{ku}, and (iv) Skewness, R_{sk}, or their surface extended parameters: S_a, S_q, S_{ku}, S_{sk}, is known. Very briefly, R_a is the arithmetic mean absolute values of the contour height deviation from the median line in the sampling length. The root mean square roughness is defined as

Table 2
Abbreviations used to identify the pretreated samples.

Acronym	Description of the sample
LM	mechanical lapped
LM10	mechanical lapped and chemical etched in 0,15M HCl for 10 s
LM30	mechanical lapped and chemical etched in 0,15M HCl for 30 s
LM60	mechanical lapped and chemical etched in 0,15M HCl for 60 s

the square root of the mean of all height values after they have been squared. The Kurtosis is a measure of contour sharpness. If the amplitude distribution curve has a Gaussian equilibrated shape, R_{ku} is equal to 3; an irregular shaped surface will give a value of R_{ku} less than 3 and a peaky or pointed surface will show R_{ku} greater than 3. The Skewness is a measure of the symmetry of the median line profile. This parameter indicates whether the tips on the surface are predominantly negative or positive or if the contour has a uniform distribution of peaks and valleys. The negative values of S_{sk} will indicate that the surface will have a good "wettability" that can promote the coating adhesion (so that the valleys determine the shape of the surface if compared to number and height of peaks). By analyzing the values assumed by the proposed roughness parameters, it is possible to obtain a numerical description of the surface, which allows choosing the structure that facilitates the substrate/coating adhesion.

2.2. Polydopamine film

The polydopamine film was obtained by dipping the samples in the aqueous solution containing 2 mg/ml of dopamine hydrochloride and 10 mM of Trizma base, for a duration of 24 hours, stirred at 500 rpm. The measured pH was 8.5. At the end of treatment, the samples were rinsed by using deionized water and cured at 150 °C for 10 minutes [34,35].

2.3. Organic coating

Epoxy coated samples were produced by using doctor blade technique (Gardco, Florida, USA) and cured in an oven at 150 °C for 10 minutes. The use of the epoxy material is not usual in the biomedical field, in fact, habitually, other polymers, like PCL or PLA, are applied. As mentioned previously, the degradation of the biomaterials is catalyzed by the pH established during the Mg oxidation. This occurrence, in turn, further increases the Mg corrosion rate due to the H_2 evolution. To test the effectiveness of the intermediate layer of PDOPA, a water-based epoxy resin (Sikkens Wapex 660, Torino, Italy), without anticorrosive pigments, has been chosen to coat the samples. The epoxy resins are stable in a wide range of pH and degrade much slower than the biodegradable materials, when exposed to Hank's solution. So that, the influence of the PDOPA layer on the variation of Mg corrosion rate can be analyzed excluding the effect of the organic coating degradation.

The specimens pretreated by using HCl solution for 10 s and coated with a layer of polydopamine have been indicated as LMP, while the specimens pretreated and covered with the organic coating have been labelled as LME, finally, the specimens pretreated and covered with the polydopamine film and, then, with the organic coating have been indicated as LMPE. The sample mechanical lapped and chemical etched for 10 s (the reason is reported in the Results and discussion paragraph) was used as a benchmark. The acronyms used are reported in Table 3.

Table 3
Abbreviations of investigated samples.

Acronym	Description of the sample
LM10	Mechanical lapped and chemical etched in 0,15M HCl for 10 s
LMP	As LM10 and PDOPA coated
LME	As LM10 and epoxy resin coated
LMPE	As LM10, coated by PDOPA and epoxy resin

2.4. Instrumentation

The surface morphology and the chemical composition of the samples were studied using the Scanning Electron Microscope (SEM) (Hitachi TM3000, Hitachi, Japan), equipped with the Energy Dispersive Spectroscopy (EDS) system (Oxford Instruments Swift ED3000). A confocal microscope DCM-3D (Leica Microsystems Srl, Milano, Italy) was employed to analyze roughness parameters. Thickness measurements of coatings were performed with a thickness gauge (Fisher MP0R-F, IMCD Italia Spa, Italy). The wettability of samples was evaluated by static contact angle test, at the temperature of 25 °C by using the sessile drop method and choosing a water drop volume of 3.5 µL. The test was carried out with a contact angle analyzer OCA15EC (DataPhysics Instruments GmbH, Filderstadt, Germany). The coating bonding strength was evaluated by tape test by using a Cross-Cut Hatcher, (Sheen Instruments, Molesey, UK) following the ASTM standard D3359-17, test method B: cross-cut tape test [36]. The electrochemical properties of samples were analyzed by potentiodynamic polarization test and electrochemical spectroscopy impedance (EIS), following ISO17475:2005 [37] and ISO16773:2016 [38], respectively. A conventional three-electrodes electrochemical cell, including a saturated calomel electrode (SCE) as a reference electrode, a platinum electrode as a counter electrode and the tested samples as working electrode, was employed. The exposed area of samples was 2.83 cm^2. Electrochemical tests were conducted in Hank's solution (Carlo Erba Reagents, Milano, Italy) at 37 °C ± 0.5 °C. Before measurements, the open circuit potential (OCP) was recorded for 90 minutes. The potentiodynamic polarization tests were performed by using the Solartron 1286 potentiostat (Photo Analytical Srl, Milano, Italy), starting from -0.01 V vs. OCP to +0.5 V vs. OCP and applying a scanning rate of 0.166 mV/s. EIS analysis were conducted by means of the Gamry Interface 1000 (Gamry Instruments, Pennsylvania, USA) imposing a sinusoidal potential of 10 mV in the frequency range of 100 kHz to 0.02 Hz. The software used to fit the experimental EIS data was Zview 2.1b (Scribner Associates Inc., North Carolina, USA). All measurements were performed three times to ensure the repeatability of the tests.

3. Results and discussion

3.1. Morphological analysis

The morphological analysis was conducted on magnesium alloys AZ31 samples, after each pretreatment, to investigate their influence on the surface topography. As can be seen in Fig. 2, reporting the SEM images acquired for lapped and etched samples, the LM sample (Fig. 2a) was characterized by the presence of small pits, as resulted in the removal of the corrosion products, while the etched samples showed a more

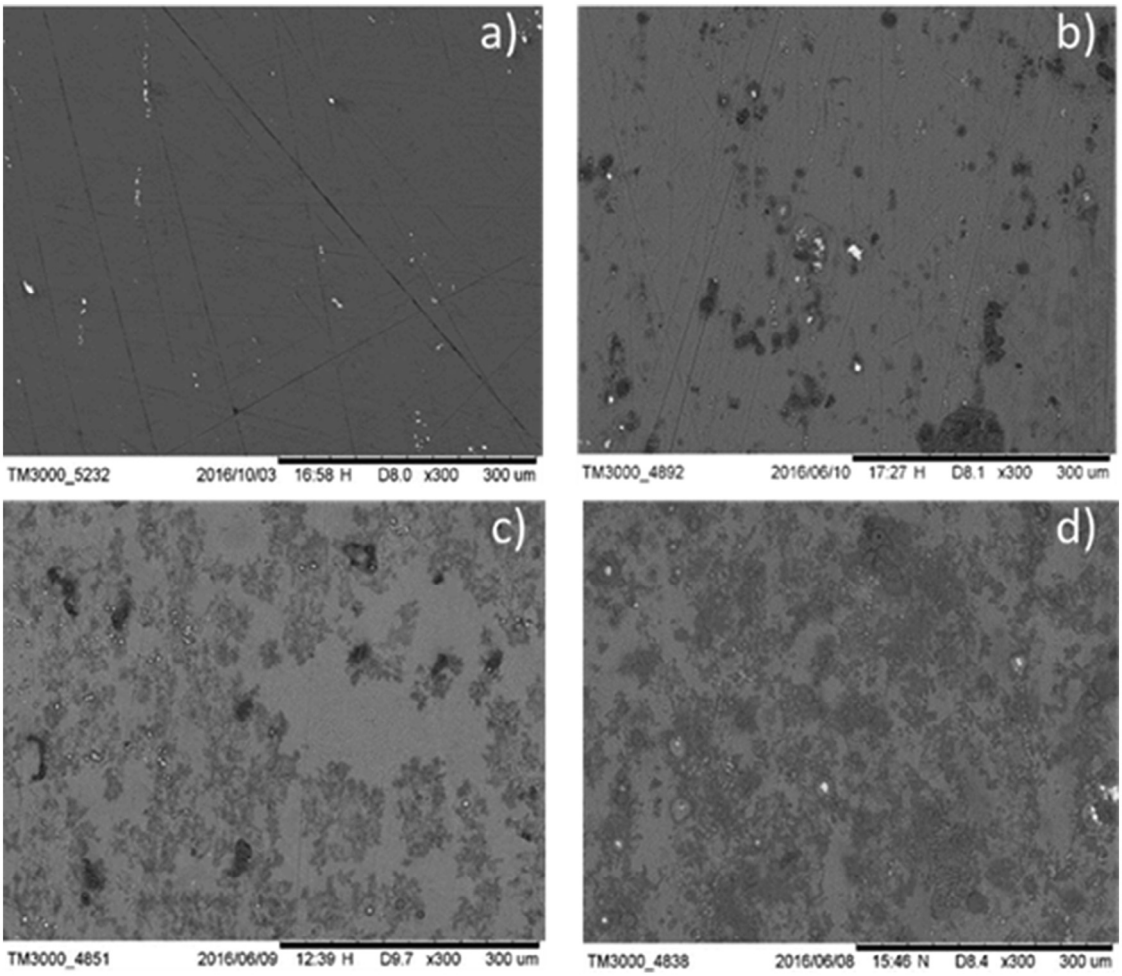

Fig. 2. Morphological analysis of samples a) mechanical lapped (LM), b) mechanical lapped and chemical etched on a 0.15M HCL aqueous solution for 10 s (LM10), c) mechanical lapped and chemical etched on a 0.15M HCL aqueous solution for 30 s (LM30) and d) mechanical lapped and chemical etched on a 0.15M!HCL aqueous solution for 60 s (LM60).

rugged surface as the acidic treatment duration increases (Fig. 2b–d).

The results obtained to study the shape of the sample's surface, by using the roughness parameters S_a, S_q, S_{sk} and S_{ku}, are reported in Table 4. They showed that: (i) the parameter S_a for LM sample assumes the lowest measured value, while the etched samples show progressively higher S_a values with increasing the immersion time, (ii) the value of S_{sk} becomes more positive with increasing the etching time and (iii) the S_{ku} value decreases when the immersion time in the HCl solution increases. In the case under study, the aim is to obtain a topography that allows a good adhesion between the metallic substrate and the coating. The parameters to be considered should be S_{sk} and S_{ku}: the first one have to be negative and the second one greater than 3. Analyzing the data reported in Table 4, the samples LM30 and LM60 showed positive values of S_{sk} (in this case can be said that the surface shape is characterized by the presence of the high number of peaks rather than valleys), so that they can be eliminated. The samples LM and LM10 showed similar values of S_a, while the first exhibited a very high value of S_{ku}, meaning that this sample possessed very high peaks in comparison to the rest of its surface. The sample LM10, between those studied, showed the best distribution of peaks and valleys and an average roughness not very dissimilar from LM and LM30 samples, for these reasons it has been chosen to be covered by the PDOPA and polymeric resin.

Table 4
Roughness parameters of pretreated samples.

Sample	S_a, µm	S_q, µm	S_{sk}	S_{ku}
LM	0,19	0,28	−3,28	32,94
LM10	0,22	0,31	−2,39	18,61
LM30	0,28	0,35	0,20	3,67
LM60	0,55	0,82	0,46	1,65

Pictures of specimens named LM10, LMP, LME and LMPE are reported in Fig. 3. As can be seen, the LMP sample is completely covered by the PDOPA film.

The measurement of the thickness of PDOPA coating revealed that the variation in color (dark gray and pale gray), that can be seen in the Fig. 3b, is due to the change in the coating thickness, its average value was found to be 4.5 µm ± 1 µm. Lee et al. [39] reported that the thickness of the PDOPA

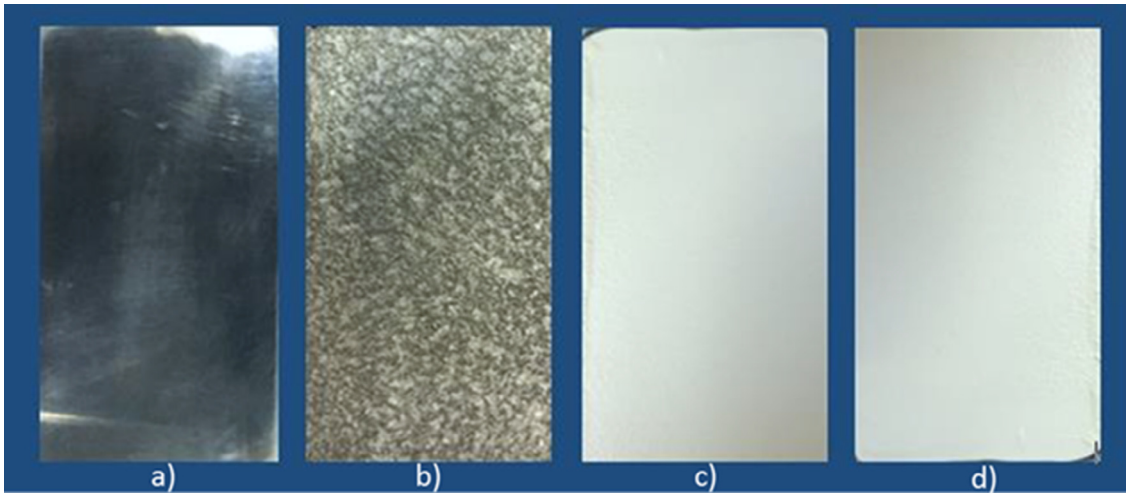

Fig. 3. Pictures of a) sample pretreated in a 0.15M HCL aqueous solution for 10 s (LM10), b) sample covered by a polydopamine layer (LMP), c) sample covered by an organic coating (LME) and d) sample pretreated and covered with a polydopamine layer and an external organic coating.

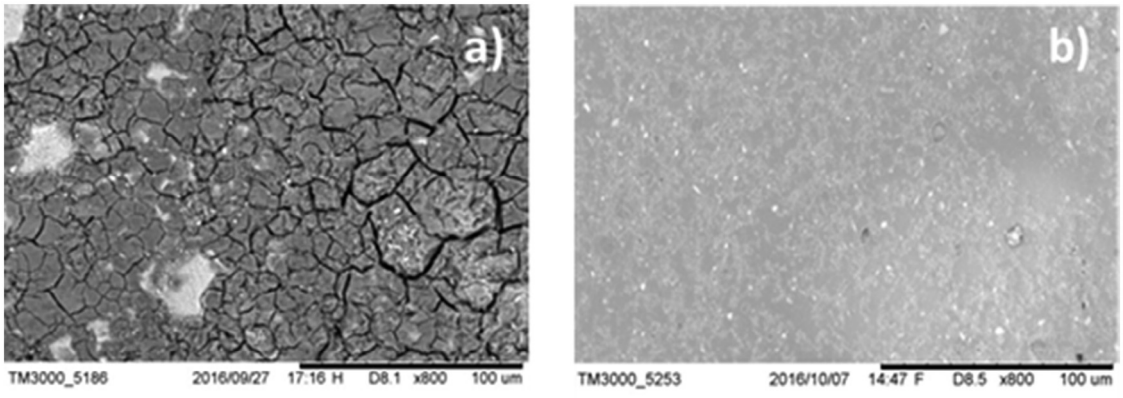

Fig. 4. SEM observation of the a) sample covered by a polydopamine layer (LMP) and b) sample covered by an organic coating (LME).

is function of the immersion time. In this study it was observed that the coating thickness is affected, also, by the rotation rate, in fact, different thicknesses were measured modifying the rotation rate or changing the dimension of magnetic anchor generating the rotation (data not reported). The SEM observations of the LMP sample (Fig. 4a) has highlighted the presence of areas in which the PDOPA appeared to be cracked; this evidence could be addressed to the coating drying, that, when losing the solvent, is affected by a decrease in volume causing material cracking. The cracked areas were associated with regions of the surface in which the thickness of the PDOPA layer possessed higher thickness than the surrounding. In the other hand, the epoxy coating (Fig. 4b) appears to be uniformly distributed over the sample surface indicating a thickness of 40 μm ± 2 μm.

3.2. Chemical analysis

The chemical analysis of the fresh prepared LM10 sample, carried out by using EDS and reported in Fig. 5, showed a chemical composition (see the Table 5) compatible with the AZ31 nominal composition.

The EDS analysis conducted on both, dark gray and pale gray, areas of the LMP sample (Figs 6 and 7) confirmed that its change in color is due to the variation of the thickness of the deposited PDOPA coating. In fact, the chemical composition of analyzed volume (reported in the Tables 6 and 7) showed that both areas are constituted of about the same amount of C, while the amount of Mg found in the dark sample area was about 1/3 times lower than that found in the lighter zone, while the amounts of N and O were lower in the pale grey area. These results highlighted that the lighter areas are covered by a smaller thickness of the PDOPA coating.

Table 5
Surface chemical composition of the LM10 sample.

Element	Weight %	Weight % σ	Atomic %
Magnesium	96.22	0.16	97.19
Aluminium	2.58	0.09	2.35
Iron	0.15	0.09	0.07
Zinc	1.05	0.09	0.39

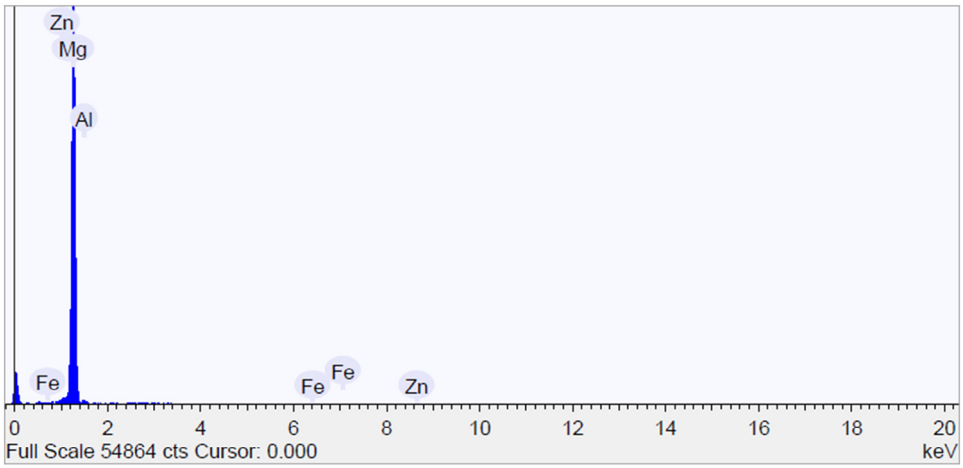

Fig. 5. EDS spectrum of the LM10 sample (AZ31 specimen pretreated in a 0.15M HCL aqueous solution for 10 s).

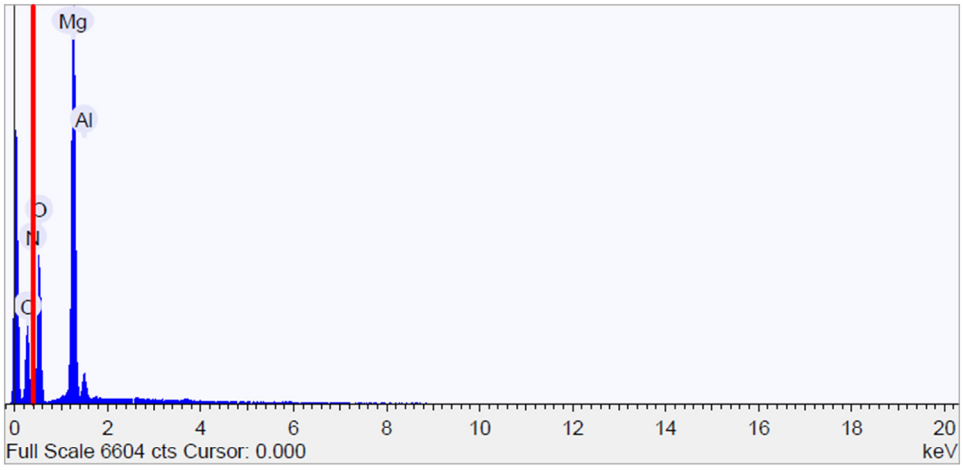

Fig. 6. Spectrum EDS in the dark areas of sample covered by polydopamine layer, LMP.

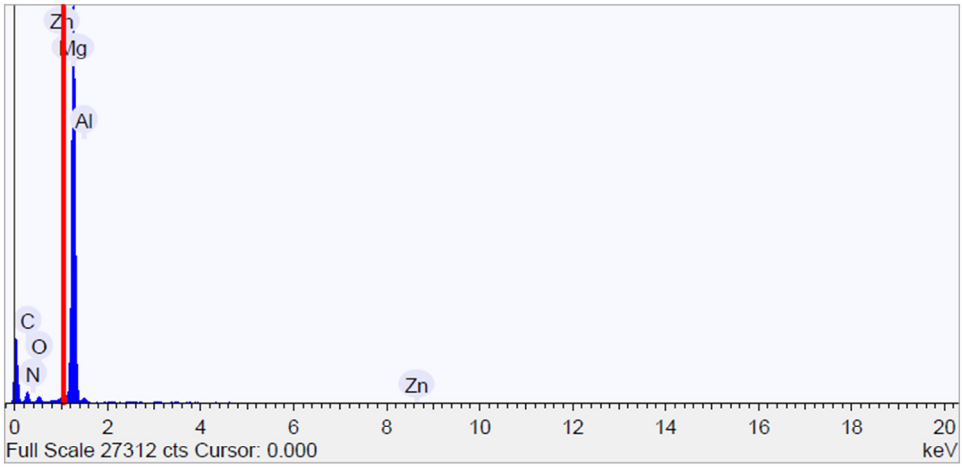

Fig. 7. EDS spectrum of the pale gray area of sample covered by polydopamine layer, LMP.

Table 6
Surface chemical composition of the dark area of the LMP sample.

Element	Weight %	Weight % σ	Atomic %
Carbon	30.40	0.56	39.31
Nitrogen	6.74	1.04	7.47
Oxygen	39.82	0.58	38.63
Magnesium	21.46	0.31	13.70
Aluminium	1.58	0.06	0.91

Table 7
Surface chemical composition of the pale gray area of the LMP sample.

Element	Weight %	Weight % σ	Atomic %
Carbon	29.87	0.628	45.16
Nitrogen	1.29	0.843	1.68
Oxygen	6.27	0.237	7.11
Magnesium	60.03	0.727	44.83
Aluminium	1.29	0.063	0.87
Zinc	1.25	0.101	0.35

Table 8
Water contact angle of the characterized samples.

Sample	LM10	LMP	LME	LMPE
Water contact angle (degree)	49	96	73	73
Standard deviation	4	3	5	3

3.3. Wettability analysis

It is well known that the contact angle measurements are difficult to perform due to several causes of error (i.e. roughness of the sample, evaporation of the liquid used, adsorption in the sample and so on) [40]. The results of measurements, carried out on the samples, are reported in Table 8, in terms of mean and standard deviation of the water contact angle (WCA) produced by the water droplet and the substrate. They are the average values obtained by 22 measurements on 5 coupons for each sample. Representative images of water droplet lied down on the substrate surface, are reported in Fig. 8. Results obtained showed the poor wettability of LMP (WCA equal to 96°), and that the bare sample exhibited a WCA of 49°, while the epoxy coating formed a WCA equal to 73°.

3.4. Adhesion test

The pictures of samples tested are reported in the Fig. 9. The LMP (Fig. 9a,b) showed no delamination after the cross-cut test, highlighting the good adhesion between the PDOPA and the base metal. This sample was rated 5B. The sample LME exhibited a partial delamination when the incisions were performed (Fig. 9c). After the tape detachment from the sample, a larger amount of resin was removed from the surface (Fig. 9d). In both cases, the detachment occurred at the polymeric coating/PDOPA interface. This sample has been rated 2B. The LMPE coupon displayed a better behavior, in fact, tiny fragments of resin were detached when the cuts were produced (Fig. 9e), no more delamination was detected after the tape test (Fig. 9f). This sample was rated 4B. The data obtained from adhesion tests collected on samples LMP, LME and LMPE, have been demonstrated that the PDOPA can be effectively utilized as an adhesion promoter in epoxy coated AZ31 system.

3.5. Electrochemical analysis

The potentiodynamic polarization curves obtained by testing the samples in Hank's solution are shown in Fig. 10, while the OCP and the current density of corrosion values are reported in Table 9.

As can be seen from Fig. 10, a synergistic effect exists when the sample is covered by, both, the PDOPA and the organic film. In fact, the LM10 bare sample exhibited a very high corrosion rate (6.2×10^{-3} A/cm^2), typical of Mg alloys in aerated aqueous saline solution [41]. When the sample is covered by the epoxy coating (LME sample), the shape of the curve is similar to LM10 sample, showing an initial kinetic regulated behavior followed by a diffusion controlled phase, but the current density value decreases of about 2 orders of magnitude, due to the protective effect of the polymeric coating. When the sample is coated by using a single layer of PDOPA (LMP specimen), a new effect is shown by the potentiodynamic test. The OCP assumes about the same value seen before but the anodic current is lower than the un-coated sample. When the specimen reaches the potential of about −1.42 V, the current sharply increases of two orders of magnitude, reaching a value similar to the un-coated sample. Even if the described behavior could be regarded as those shown by "passive" layers, the current density is too high and the extent of the range of "passivity" is very narrow to conjecture the formation of a passive layer on sample [26].

Table 9
OCP and current density of corrosion values of the investigated samples.

Sample	LM10	LMP	LME	LMPE
OCP (V vs. SCE)	−1.56	−1.47	−1.55	−1.55
|i| (A/cm^2)	6.2×10^{-3}	8.1×10^{-5}	9.5×10^{-5}	7.6×10^{-7}

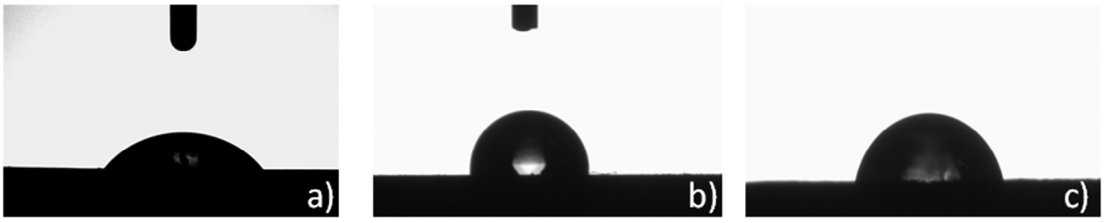

Fig. 8. Pictures of the water contact angle on a) LM10 sample, b) LMP sample and c) LME sample.

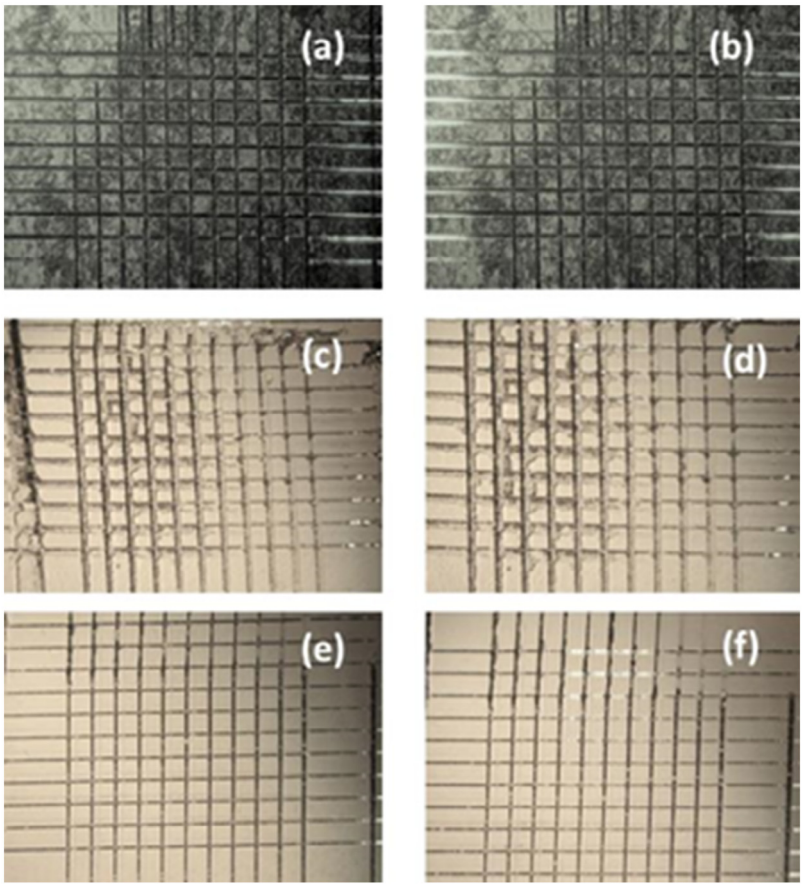

Fig. 9. Cross-cut test on LMP sample, a) before and b) after the test, on LME sample, c) before and d) after the test, on LMPE sample, e) before and f) after the test.

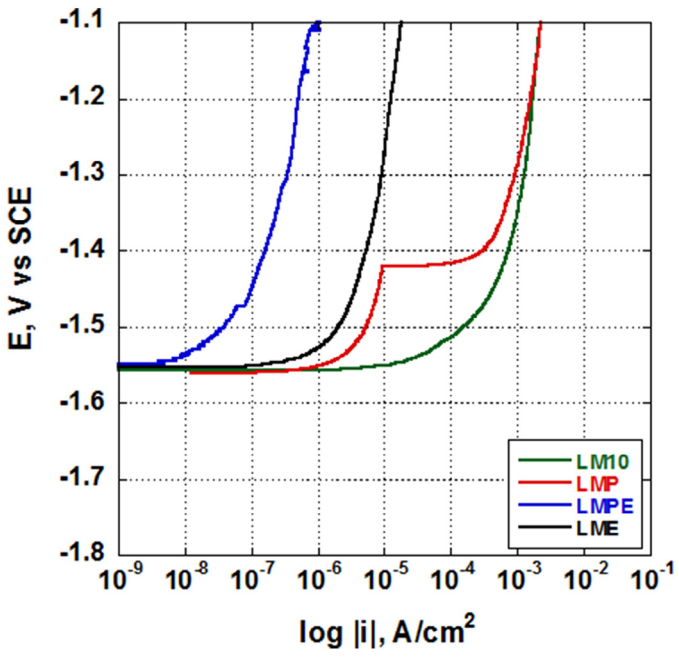

Fig. 10. Potentiodynamic curve of the investigated sample when exposed to Hank's solution.

The proposed mechanism to explain the behavior of LMP sample is the following: the surface of the PDOPA coated sample, is not uniform, the SEM picture shows an extended area with crevices (see Fig. 4a), so the sharp increases of the current can be addressed to the intensification of H_2 evolution rate that determined a widening of the anodic areas, caused by the delamination of the PDOPA layer, that further produced the increase of H_2 evolution.

The potentiodynamic data acquired for the sample LMPE, that is covered by both the PDOPA and epoxy layers (Fig. 10), showed a decrease in current density compared to the other samples, until reaching a value equal to 7.6×10^{-7} A/cm^2, displaying that: (i) the intermediate layer of PDOPA possesses beneficial effects reducing the overall corrosion rate of magnesium and (ii) the polymeric coating protects the PDOPA under layer, eliminating the "pseudo-passive" behavior described above. On the other hand, although the PDOPA formed another layer in the system, it should be considered that its thickness was of about 4.5 μm and that the coating showed several defects, so that the behavior exhibited by the sample LMPE cannot be justified considering, merely, the sum of the effects caused by the presence of the PDOPA and the epoxy resin. In fact, it is conceivable that the reduction of the corrosion rate of

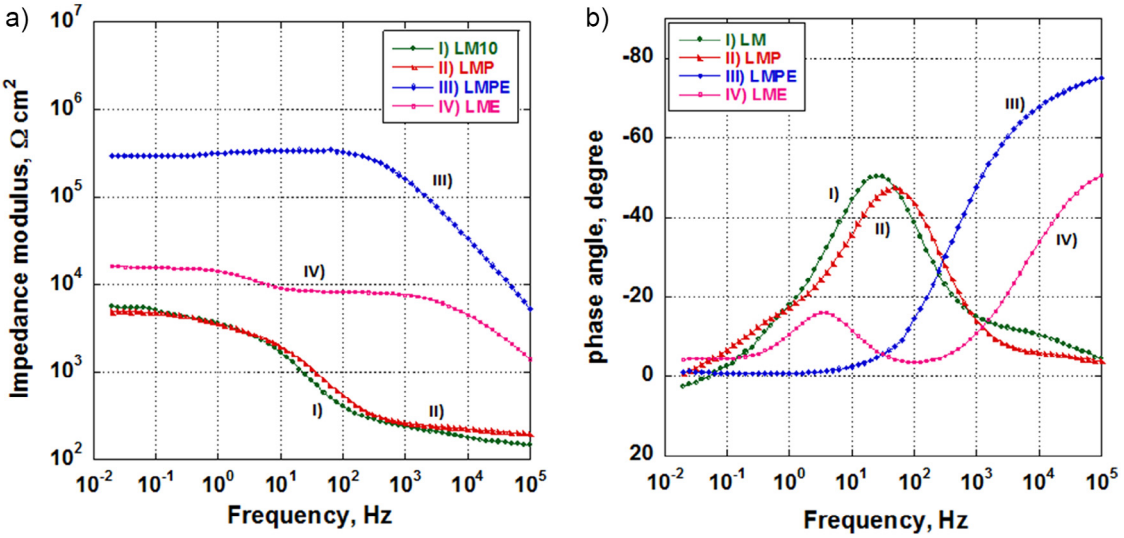

Fig. 11. a) Impedance modulus and b) phase angle of the investigated sample when exposed to Hank's solution.

the system LMPE cannot be attributed to the presence of an additional layer but to the procured effect due to the interaction between PDOPA/metallic substrate and between PDOPA/epoxy coating.

The EIS data obtained characterizing the LM10, LMP, LME and LMPE samples, represented in Fig. 11, confirmed the effectiveness of the PDOPA as an intermediate layer in the AZ31/polymeric coating system. In fact, the experimental results highlighted the active behavior of bare LM10 sample when immersed in Hank's solution (curve I). The covering of the sample by using only the PDOPA layer, seemed to have no contribution to any improvement in retarding Mg dissolution, as pointed out by the curve II. The scarce barrier properties offered by the PDOPA coating due to its physical properties and, as seen in the Fig. 4a, to the cracked structure of the coating, allow the direct contact between the metallic surface and the solution. The sample LME (curve IV) exhibited a little better protective properties if compared to the bare specimen, in the same time, collected data confirmed the scarce anticorrosive properties of the polymeric coating used. The curve III permitted to underline the synergistic effect due to the use of both the PDOPA and polymeric coating, recording the highest impedance modulus value. As the data demonstrated, the total modulus of impedance exhibited by the LMPE sample is of about one order of magnitude higher than that measured for the LME sample and about due order higher than that evinced by the LMP coupon. These results confirmed that the system's increased performances could not be a simple additive consequence produced by the presence of the two coating layers, but they can be addressed to an increase of adhesion strength at the metallic/coating interface that reduces the layer's delamination, avoiding that new anodic areas being exposed, thus reducing the magnesium corrosion rate. As a consequence, a smaller amount of H_2 is produced which, in turn, induces a smaller increase in the surface broadening of the cathodic areas.

The magnesium alloy exposed to air spontaneously forms on its surface a porous oxide layer (as represented in Fig. 12a). When the metal substrate is immersed in the polydopamine solution and dried, a cracked PDOPA film is created (Fig. 12b). If, after this treatment, the specimen is covered with an organic coating, it fills the cracked PDOPA film (Fig. 12c), while, if the metal substrate is covered by the organic coating alone, this effect is not achieved (Fig. 12d).

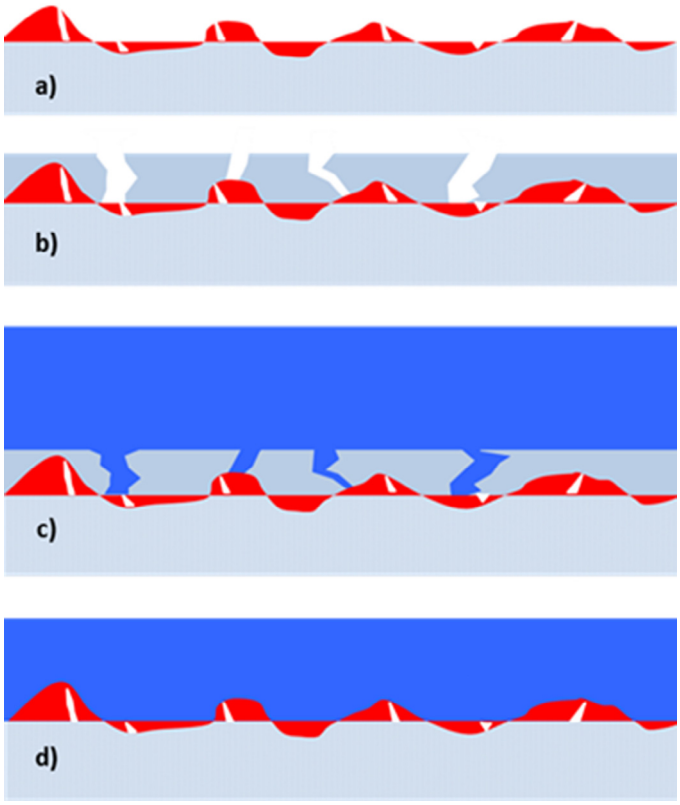

Fig. 12. Schematic representation of (a) the magnesium sample covered by the porous oxide layer spontaneously formed when exposed to air, (b) the AZ31 substrate coated by the porous PDOPA layer, (c) the sample covered by the PDOPA layer and organic coating and (d) the sample protected by the polymeric resin.

Table 10
Equivalent circuit elements values obtained by using the model reported in Fig. 13.

Sample	R_s (Ω cm^2)	CPE_c (F/cm^2)	n_c	R_c (Ω cm^2)	CPE_{dl} (F/cm^2)	n_{dl}	R_{ct}(Ω cm^2)	χ^2
LM10	135,64	3,77E-05	0,55	2,22E+02	3,30E-06	1,00	4,95E+03	0.0030
LMP	150,47	3,85E-04	0,42	1,24E+02	3,99E-06	0,93	5,19E+03	0.0015
LME	158,23	5,83E-08	0,70	8,23E+03	1,39E-05	0,87	7,55E+03	0.0025
LMPE	155,65	4,10E-09	0,80	3,59E+05	3,08E-05	0,88	2,32E+04	0.0049

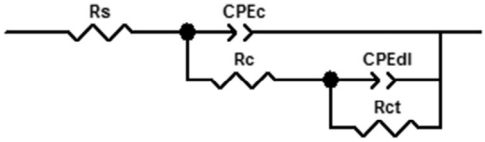

Fig. 13. Equivalent circuit proposed to simulate the electrochemical behavior of the samples when exposed to the Hank's solution.

Starting from these physical models, the simulation of the electrochemical behavior of the tested samples, was carried out by means of the equivalent circuits analysis, employing the model reported in Fig. 13, that has been widely used to study a coated metallic substrate [42–44].

In the proposed model, R_s represents the impedance of the electrolytic solution, R_{ct} is the charge transfer resistance and CPE_{dl} is the non-ideal double layer capacitance of the metallic interface. The other components assume a diverse physical meaning depending on the sample considered. In the case of the LM10 coupons R_c and CPE_c take into account of the resistance and non-ideal capacitive behavior of porous oxide layer spontaneously formed on the sample. While, when considering the sample LMP and LMPE, R_c and CPE_c take into account of the resistance and non-ideal capacitive behavior of the overall layers covering the sample, i.e. in the first case of the PDOPA porous layer, in the second of both the PDOPA and the polymeric coating.

Table 10 shows the values obtained from the fitting procedure of the samples LM10, LMP, LME and LMPE, for which the χ^2 value was found equal to 0.0030, 0.0015, 0.0025 and 0.0049, respectively, demonstrating the fitting goodness. Fitted parameters values showed that the layers covering the LM10 and LMP are, for different reasons, very porous, in fact, the n_c values are equal to 0.55 and 0.42 respectively. This feature justifies the poor protective properties exhibited by the samples just cited and impinged on the R_c values that, for both samples, assumed the values of about $1x10^2$ Ω•cm^2. At the same time, the values of the charge transfer resistance, R_{ct}, were found to be equal to about $5x10^3$ Ω•cm^2, for both samples, justified by the high reactivity of magnesium substrate. As described previously, the polymeric resin offers a little better protection to the substrate, in fact, considering the fitted values of parameters obtained for the sample LME, it can been seen that there is a small increase in the R_c and R_{ct} values due to the more compact nature of the resin covering the substrate ($n_c = 0.7$) and its chemical composition that assures a CPC_c equal to $5{,}83^{-8}$ F/cm^2. Fitted values of the parameters confirmed the synergistic effect due to the use of the PDOPA and polymeric coating when used together (sample LMPE). In fact, the CPEc value resulted one order of magnitude lower than the one estimated for the organic coating alone, the $n_c = 0.8$ indicated a more compact nature of the multilayer coating so that the R_c was equal to 3.59×10^5 Ω•cm^2 showing better protective properties, which implies a higher value of the R_{ct} that was found equal to 2.32×10^4 Ω•cm^2. Analyzing the EIS fitted data, the synergistic effect played by the organic coating/PDOPA system can be interpreted by assuming that (i) the PDOPA layer increases the adhesion at metallic substrate/organic coating interface, (ii) the cracked layer of PDOPA serves as mechanical anchoring for the organic coating further increasing its adhesion, while (iii) the organic coating seals the fissures in PDOPA layer, increasing the overall protective properties of the multilayer.

4. Conclusions

The effect of polydopamine as an intermediate layer in the epoxy resin/AZ31 system was studied. The experimental results showed that:

1 good adhesion to the metal was obtained covering the substrate by using PDOPA;
2 despite the poor wettability of PDOPA, a good adhesion at the organic coating/PDOPA interface was achieved;
3 the PDOPA layer decreases the corrosion rate of AZ31 when used together with an external organic coating;
4 the efficacy in the use of PDODA is due to the synergistic effect performed in the system under study.
5 the synergistic effect can be explained considering, both, physical and chemical interactions between the PDOPA layer and the organic coating.

Acknoweledgement

The authors would like to thank Dr. Carla Velotti for her precious contribution in the roughness measurements.

References

[1] T.A. Dantas, C.S. Abreu, M.M. Costa, G. Miranda, F.S. Silva, N. Dourado, et al., Mater. Sci. Eng. C 77 (2017) 1104–1110.
[2] S. Durdu, M. Usta, A.S. Berkem, Surf. Coat. Technol. 301 (2016) 85–93.
[3] C. Marinescu, A. Sofronia, E.M. Anghel, R. Baies, D. Constantin, A.M. Seciu, et al., Arab. J. Chem. (2017) doi:10.1016/j.arabjc.2017.01.019.
[4] T. Yu, Q. Liu, T. Jiang, X. Wang, Y. Yang, Y. Kang, Adv. Funct. Mater. 26 (37) (2016) 6719–6727.
[5] E. Beltrán-Partida, B. Valdez-Salas, M. Curiel-Álvarez, S. Castillo-Uribe, A. Escamilla, N. Nedev, Mater. Sci. Eng. C 76 (2017) 59–65.
[6] I. De Santo, L. Sanguigno, F. Causa, T. Monetta, P.A. Netti, Analyst 137 (21) (2012) 5076–5081.
[7] T. Monetta, F. Bellucci, Plasma Chem. Plasma Proces. 34 (6) (2014) 1247–1256.
[8] T. Monetta, A. Scala, C. Malmo, F. Bellucci, Plasma Med. 1 (3–4) (2011) 205–214.

[9] A. Pawlik, M. Jarosz, K. Syrek, G.D. Sulka, Colloids Surf. B Biointerfaces 152 (2017) 95–102.
[10] Q. Wang, J.Y. Huang, H.Q. Li, A.Z.J. Zhao, Y. Wang, K.Q. Zhang, et al., Int. J. Nanomedicine 12 (2017) 151–165.
[11] F. Witte, H. Ulrich, C. Palm, E. Willbold, J. Biomed. Mater. Res. A 81 (3) (2007) 757–765.
[12] F. Witte, I. Abeln, E. Switzer, V. Kaese, A. Meyer-Lindenberg, H. Windhagen, J. Biomed. Mater. Res. A 86 (4) (2008) 1041–1047.
[13] B. Lin, M. Zhong, C. Zheng, L. Cao, D. Wang, L. Wang, et al., Surf. Coat. Technol. 281 (2015) 82–88.
[14] B.M. Wilke, L. Zhang, JOM 68 (6) (2016) 1701–1710.
[15] A. Zomorodian, C. Santos, M.J. Carmezim, T.M.E. Silva, J.C.S. Fernandes, M.F. Montemor, Electrochim. Acta 179 (2015) 431–440.
[16] Y. Chen, Y. Song, S. Zhang, J. Li, C. Zhao, X. Zhang, Biomed. Mater. 6 (2) (2011).
[17] J.H. Waite, Nat. Mater. 7 (1) (2008) 8–9.
[18] A. Bourmaud, J. Riviere, A. Le Duigou, G. Raj, C. Baley, Polym. Test. 28 (6) (2009) 668–672.
[19] J.H. Waite, Integr. Comp. Biol. 42 (6) (2002) 1172–1180.
[20] Z. Liu, S. Qu, J. Weng, Prog. Chem. 27 (2–3) (2015) 212–219.
[21] X. Liu, J. Cao, H. Li, J. Li, Q. Jin, K. Ren, et al., ACS Nano 7 (10) (2013) 9384–9395.
[22] W.B. Tsai, W.T. Chen, H.W. Chien, W.H. Kuo, M.J. Wang, J. Biomater. Appl. 28 (6) (2014) 837–848.
[23] J. Park, T.F. Brust, H.J. Lee, S.C. Lee, V.J. Watts, Y. Yeo, ACS Nano 8 (4) (2014) 3347–3356.
[24] Y. Chen, S. Zhao, M. Chen, W. Zhang, J. Mao, Y. Zhao, et al., Corros. Sci. 96 (2015) 67–73.
[25] L. Huang, J. Yi, Q. Gao, X. Wang, Y. Chen, P. Liu, Surf. Coat. Technol. 258 (2014) 664–671.
[26] F. Singer, M. Schlesak, C. Mebert, S. Höhn, S. Virtanen, ACS Appl. Mater. Interfaces 7 (48) (2015) 26758–26766.
[27] C. Wang, J. Shen, F. Xie, B. Duan, X. Xie, Corros. Sci. 122 (2017) 32–40.
[28] P. Tian, D. Xu, X. Liu, Colloids Surf. B Biointerfaces 141 (2016) 327–337.
[29] K. Geels, D.B. Fowler, W.-U. Kopp, M. Rückert. Metallographic and Materialographic Specimen Preparation, Light Microscopy, Image Analysis, and Hardness Testing. 2007.
[30] M. Sedlacek, P. Gregorcic, B. Podgornik, Tribol. Trans. 60 (2) (2017) 260–266.
[31] T. Monetta, A. Acquesta, F. Bellucci, Metal. Ital. 106 (9) (2014) 13–21.
[32] T. Monetta, G. Marchesano, F. Bellucci, G. Lupo, A. Itro, Dent. Cadmos 82 (7) (2014) 498–508.
[33] A. Scala, A. Squillace, T. Monetta, D.B. Mitton, D. Larson, F. Bellucci, Surf. Interface Anal. 42 (4) (2010) 194–198.
[34] C.C. Ho, S.J. Ding, J. Biomed. Nanotechnol. 10 (10) (2014) 3063–3084.
[35] Q. Ye, F. Zhou, W. Liu, Chem. Soc. Rev. 40 (7) (2011) 4244–4258.
[36] ASTM D3359-17 Standard Test Methods for Measuring Adhesion by Tape Test, 2017.
[37] ISO17475: 2005 Corrosion of metals and alloys – Electrochemical test methods – Guidelines for conducting potentiostatic and potentiodynamic polarization measurements – First Edition. 2005.
[38] ISO 16773: 2016 Electrochemical impedance spectroscopy (EIS) on coated and uncoated metallic specimens. 2016.
[39] H. Lee, S.M. Dellatore, W.M. Miller, P.B. Messersmith, Science 318 (5849) (2007) 426–430.
[40] J.A. Nychka, M.M. Gentleman, JOM 62 (7) (2010) 39–48.
[41] G. Song, S. Song, Adv. Eng. Mater. 9 (4) (2007) 298–302.
[42] G.W. Walter, Corros. Sci. 32 (10) (1991) 1041–1058.
[43] E.P.M. van Westing, G.M. Ferrari, J.H.W. De Wit, Electrochim. Acta 39 (7) (1994) 899–910.
[44] C. Bitondo, A. Bossio, T. Monetta, M. Curioni, F. Bellucci, Corros. Sci. 87 (2014) 6–10.